Biogeosciences, 18, 4305–4320, 2021
https://doi.org/10.5194/bg-18-4305-2021

Biogeosciences
Open Access
EGU

Nitrogen loss processes in response to upwelling in a Peruvian coastal setting dominated by denitrification – a mesocosm approach

Kai G. Schulz[1], Eric P. Achterberg[2], Javier Arístegui[3], Lennart T. Bach[4], Isabel Baños[3], Tim Boxhammer[2], Dirk Erler[1], Maricarmen Igarza[5], Verena Kalter[2,6], Andrea Ludwig[2], Carolin Löscher[7], Jana Meyer[2], Judith Meyer[2], Fabrizio Minutolo[2], Elisabeth von der Esch[8], Bess B. Ward[9], and Ulf Riebesell[2]

[1]Centre for Coastal Biogeochemistry, School of Environment, Science and Engineering, Southern Cross University, Lismore, NSW, Australia
[2]GEOMAR Helmholtz Centre for Ocean Research Kiel, Kiel, Germany
[3]Instituto de Oceanografía y Cambio Global, IOCAG, Universidad de Las Palmas de Gran Canaria ULPGC, Las Palmas, Spain
[4]Institute for Marine and Antarctic Studies, University of Tasmania, Hobart, Tasmania, Australia
[5]Instituto del Mar del Perú (IMARPE), Dirección General de Investigaciones en Oceanografía y Cambio Climático, Callao, Peru
[6]Department of Ocean Sciences, Memorial University of Newfoundland, Logy Bay, Newfoundland, Canada
[7]Department of Biology, Nordcee, Danish Institute for Advanced Study (DIAS), University of Southern Denmark, Campusvej 55, Odense M, Denmark
[8]Institute of Hydrochemistry, Chair of Analytical Chemistry and Water Chemistry, Technical University of Munich, Munich, Germany
[9]Department of Geosciences, Princeton University, Princeton, New Jersey 08544, USA

Correspondence: Kai G. Schulz (kai.schulz@scu.edu.au)

Received: 14 January 2021 – Discussion started: 18 January 2021
Revised: 15 June 2021 – Accepted: 26 June 2021 – Published: 23 July 2021

Abstract. Upwelling of nutrient-rich deep waters make eastern boundary upwelling systems (EBUSs), such as the Humboldt Current system, hot spots of marine productivity. Associated settling of organic matter to depth and consecutive aerobic decomposition results in large subsurface water volumes being oxygen depleted. Under these circumstances, organic matter remineralisation can continue via denitrification, which represents a major loss pathway for bioavailable nitrogen. Additionally, anaerobic ammonium oxidation can remove significant amounts of nitrogen in these areas. Here we assess the interplay of suboxic water upwelling and nitrogen cycling in a manipulative offshore mesocosm experiment. Measured denitrification rates in incubations with water from the oxygen-depleted bottom layer of the mesocosms (via ^{15}N label incubations) mostly ranged between 5.5 and 20 nmol N_2 L^{-1} h^{-1} (interquartile range), reaching up to 80 nmol N_2 L^{-1} h^{-1}. However, actual in situ rates in the mesocosms, estimated via Michaelis–Menten kinetic scaling, did most likely not exceed 0.2–4.2 nmol N_2 L^{-1} h^{-1} (interquartile range) due to substrate limitation. In the surrounding Pacific, measured denitrification rates were similar, although indications of substrate limitation were detected only once. In contrast, anammox (anaerobic ammonium oxidation) made only a minor contribution to the overall nitrogen loss when encountered in both the mesocosms and the Pacific Ocean. This was potentially related to organic matter C / N stoichiometry and/or process-specific oxygen and hydrogen sulfide sensitivities. Over the first 38 d of the experiment, total nitrogen loss calculated from in situ rates of denitrification and anammox was comparable to estimates from a full nitrogen budget in the mesocosms and ranged between ~ 1 and 5.5 µmol N L^{-1}. This represents up to $\sim$ 20 % of the initially bioavailable inorganic and organic nitrogen standing stocks. Interestingly, this loss is comparable to the total amount of particulate organic nitrogen that was exported into the sediment traps at the bottom of the mesocosms at about 20 m

depth. Altogether, this suggests that a significant portion, if not the majority of nitrogen that could be exported to depth, is already lost, i.e. converted to N_2 in a relatively shallow layer of the surface ocean, provided that there are oxygen-deficient conditions like those during coastal upwelling in our study. Published data for primary productivity and nitrogen loss in all EBUSs reinforce such conclusion.

1 Introduction

Amongst the most productive marine ecosystems are eastern boundary upwelling systems (EBUSs), which are mainly fuelled by the wind-driven upwelling of dissolved inorganic nutrient-rich deep waters to the surface ocean, stimulating primary and associated higher trophic level productivity (Chavez and Messié, 2009; Kämpf and Chapman, 2016; FAO, 2018). This is particularly true for the Humboldt Current system off Peru (Montecino and Lange, 2009). High productivity and the eventual export of organic matter to depth result in marked oxygen consumption by aerobic respiration, leading to so-called subsurface oxygen-depleted zones and virtually anoxic oxygen minimum zones (ODZs and OMZs, respectively) at depth (e.g. Cline and Richards, 1972; Paulmier and Ruiz-Pino, 2009). In the absence of oxygen, heterotrophic organic matter decomposition can continue with alternative electron acceptors, such as nitrate (NO_3^-) or nitrite (NO_2^-) via nitric oxide (NO) and nitrous oxide (N_2O) to molecular nitrogen (N_2), in a series of separate steps carried out by a variety of bacteria (Zumft, 1997). In their entirety, these processes are summarised as denitrification. A by-product of denitrification is ammonium (NH_4^+) from remineralised organic matter, but overall denitrification constitutes a net loss of bioavailable nitrogen (Paulmier et al., 2009). A second prevalent nitrogen loss pathway in ODZs and OMZs is autotrophic anaerobic ammonium oxidation (anammox) which utilises NH_4^+ and NO_2^- produced by heterotrophic processes to produce energy for carbon dioxide (CO_2) fixation and organic matter production (Thamdrup et al., 2006; Brandes et al., 2007).

Observational and modelling studies have estimated the loss of bioavailable nitrogen via water column denitrification and anammox in suboxic ODZs and anoxic OMZs to amount to about 20 %–35 % of the total nitrogen losses ocean-wide (for reviews, see Bianchi et al., 2012; Zhang et al., 2020). In a context of climate/ocean change, which has been projected to enhance the temperature gradient between land and ocean and, hence, alongshore winds (Di Lorenzo, 2015), upwelling intensity, and the frequency of deep waters would subsequently increase (Hauri et al., 2013; Wang et al., 2015). Such a scenario has been put forward for the Humboldt Current system off Peru but also other EBUSs (Bakun and Weeks, 2008; Varela et al., 2015). Furthermore, due to increasing temperatures, the ocean loses oxygen (O_2), and OMZs are expanding (e.g. Bopp et al., 2002; Bograd et al., 2008; Stramma et al., 2008; Oschlies et al., 2017). Together with changes in microbial activity, this modifies the biogeochemical properties of upwelled waters, including, next to O_2, carbonate chemistry speciation, i.e. ongoing ocean acidification further decreases already low deep water pH levels (e.g. Feely et al., 2008; Franco et al., 2018; Schulz et al., 2019). Changes in the upwelling frequency and/or intensity, oxygen availability, temperature, and pH could influence planktonic food web functioning in EBUSs, with repercussions for nitrogen loss processes.

To better understand the events following the coastal upwelling of oxygen- and nitrogen-depleted deep waters, we make use of an offshore mesocosm set-up. This approach allows the simulating of upwelling and the tracing of biogeochemical element cycling, as well as associated trophic interactions. We were specifically aiming to address the question of nitrogen cycling, i.e. the build-up and turnover of organic nitrogen pools, their export from the surface to depth, and, most importantly, potential loss processes. Because such an approach enables budgeting of the various pools, it will be an alternative and independent assessment of the nitrogen balance in coastal ODZs next to classical shipboard transects.

2 Methods

The current experiment started on 22 February 2017 with the deployment of eight Kiel Off-Shore Mesocosms for Future Ocean Simulations (KOSMOS) about 4 nautical miles (nm) off the Peruvian coast, close to San Lorenzo Island at 12.0555° S and 77.2348° W, and ended on 16 April 2017 after 50 d of sampling. Full details on the experimental set-up, the sampling, manipulation, and maintenance schedule can be found in Bach et al. (2020a).

2.1 Mesocosm set-up and sampling

The KOSMOS system comprised eight mesocosms consisting of polyurethane bags 2 m in diameter extending to $\sim$ 18.7 m depth, with the last 2 m being a funnel-shaped sediment trap. After 2 d of thorough flushing and soaking of the bags, which had been pulled under the surface and were open to water exchange through a 3 mm mesh on both ends, the bags were secured above the water line, and the sediment traps were attached, enclosing about 54 m^3 of a natural plankton assemblage. Sampling commenced on 26 February, i.e. day 1. Sampling days typically started in the morning between 06:30–07:00 PET (Peru time) by removing the material that had accumulated in the sediment traps with a pump, followed by CTD (conductivity, temperature, and depth) casts. The CTD (Sea & Sun Technology 90M memory probe) was additionally equipped with an optical oxygen sensor and a calibrated AMT (Analysenmesstechnik GmbH, Germany) amperometric hydrogen sulfide (H_2S) sensor (for details on

the operation, the other sensors, and calibrations/corrections, see Schulz and Riebesell, 2013). CTD casts were followed by sampling with an integrating water sampler (IWS; HydroBios). Because strong thermal stratification resulted in two distinct water masses at the surface (high oxygen and pH) and at the bottom (low oxygen and pH) of the mesocosms (Fig. 2a, b and c), two separate depth-integrated water samples were taken. According to changes in stratification, the depths were adjusted over time (days 1–2 – 0–5 and 5–17 m, surface and bottom, respectively; days 3–28 – 0–10 and 10–17 m, surface and bottom, respectively; days 30–50 – 0–12.5 and 12.5–17 m, surface and bottom, respectively).

Furthermore, to stabilise and maintain bottom water characteristics (as in the surrounding Pacific), a NaCl brine solution was homogeneously injected below 10 m on day 13 and below 12.5 m on day 33, increasing salinity, and, hence, stratification, by about 0.7 and 0.5 psu (practical salinity unit), respectively (see Bach et al., 2020a, for details).

While all seawater bulk parameters, such as particulate and dissolved organic matter or dissolved inorganic nutrients, were measured on the two depth-integrated samples (see Sect. 2.5 below for details), samples for N loss process incubations (see Sect. 2.3 below for details) were taken with a Niskin sampler from 15.25 m depth and treated as gas sensitive, i.e. filled into two 100 mL glass-stoppered DURAN bottles with at least one bottle volume of overflow, closed without headspace, and kept cold and in the dark ($\sim$ 2–4 h) until processing. A direct comparison of oxygen concentrations in these samples by means of Winkler titrations, following the recommendations of Carritt and Carpenter (1966); Bryan et al. (1976), and Grasshoff et al. (1983) with CTD–oxygen–optode measurements, revealed an offset by $+13\,\mu mol\,L^{-1}$ in the CTD data, although response time hysteresis had been corrected for $\tau = 1$ s, as described in Fiedler et al. (2013). Hence, oxygen concentrations at depth, as shown here from CTD casts, are likely to have been significantly lower. The most likely explanation for this offset is that the response time of the sensor was actually slower, i.e. of the order of 2–2.5 s.

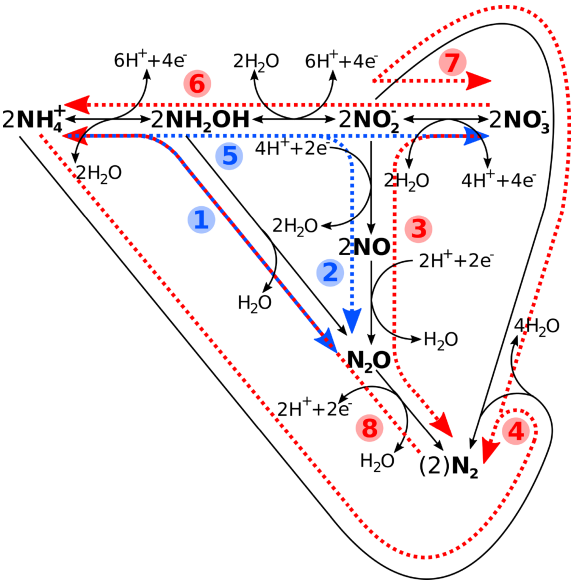

Figure 1. Schematic reaction diagram of major marine nitrogen cycling processes, with (1) hydroxylamine oxidation, (2) nitrifier denitrification, (3) denitrification, (4) anammox, (5) nitrification, (6) nitrate ammonification (DNRA), (7) anaerobic nitrite oxidation, and (8) nitrogen fixation. While processes 1–4 are considered nitrogen loss processes, 5–7 constitute neither a loss nor a gain, with (8) being the latter. Blue denotes oxic and red suboxic and/or anoxic processes. Please note that, while the reactions have been chemically balanced for electro-neutrality, the exact amount of H^+, e^-, or water produced and/or consumed will depend on the actual organism or enzyme and reaction pathway. See Bourbonnais et al. (2017), Codispoti et al. (2005), and Zumft (1997), and references therein, for details.

2.2 Deep water collection and addition

To simulate upwelling with two distinct OMZ signatures, in terms of N deficit, deep water was collected from 90 m at 12.044333° S, 77.377583° W, and 30 m at 12.028323° S, 77.223603° W, on days 5 and 10, respectively. However, both waters had quite a strong N deficit (N*) in comparison to a typical N / P of 16/1 required for phytoplankton growth (Redfield et al., 1963; Brzezinski, 1985), and will be referred to as "low N / P" and "very low N / P" treatments in the following (compare Table 1). The deep waters were collected into 100 m^3 bags, without headspace, at the respective depths and sealed once brought back to the surface. Deep water was added by first removing about 20 m^3 from each mesocosm and replacing it with the respective deep water that was injected into the bottom layer, between 14 and 17 m, on day 11, and the surface layer, between 1 and 9 m, on day 12. To minimise changes to deep water gas concentrations during injection, water was pumped from 2 m depth out of the deep water bags. For further details on collection and addition, see Bach et al. (2020a).

2.3 N loss processes incubations, measurements, and calculations

The two main N loss processes in oxygen-deficient waters off the Peruvian coast, i.e. denitrification and anammox (Fig. 1), were assayed with incubations of water from 15.25 m depth, using labelled $^{15}NH_4Cl$ ($\geq$ 98 atom %) or $Na^{15}NO_2$ (98 atom %), i.e. by an addition of $3\,\mu mol\,L^{-1}$ each. During incubations with the former, anammox will be traced by the production of $^{29}N_2$ ($^{15}N^{14}N$) and $^{30}N_2$ ($^{15}N^{15}N$) if coupled to nitrification (although unlikely as it is an oxic process; compare Fig. 1). During incubations with $^{15}NO_2^-$, anammox would again produce $^{29}N_2$, while denitrification would produce both $^{29}N_2$ and $^{30}N_2$ (Fig. 1). Here, a further complication for rate calculations would be coupled

Table 1. Concentrations of nitrate, nitrite, ammonium, dissolved organic nitrogen (DON), and dissolved organic phosphorus (DOP), and silicate (micromoles per litre, hereafter µmol L^{-1}) in the two deep water batches and associated inorganic N / P / Si in comparison to a Redfield ratio of 16/1/16 (see the text for details), and the inorganic N deficit calculated as $N^* = DIN - 16 \times PO_4^{3-}$, with DIN denoting the sum of NO_3^- NO_2^- and NH_4^+.

	NO_3^-	NO_2^-	NH_4^+	DON	PO_4^{3-}	DOP	$Si(OH)_4$	N / P / Si	N*
Low N / P DW	1.1	2.9	0.3	5.5	2.5	0.2	19.6	1.7/1/7.8	−35.7
Very low N / P DW	0	0	0.3	5.2	2.6	0.2	17.4	0.1/1/6.7	−41.3

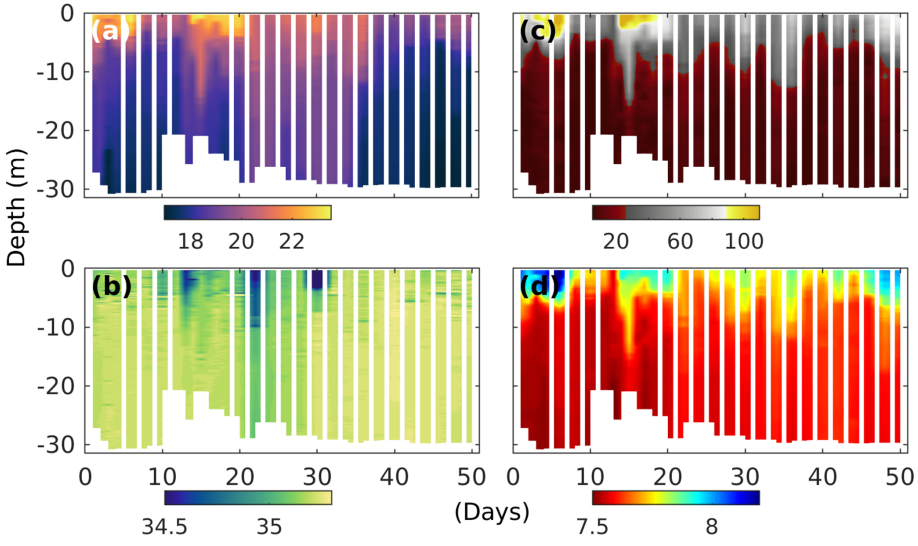

Figure 2. Temporal development of upwelling and stratification in the surrounding Pacific waters at the mooring site (water depth between 25 and 30 m), as evidenced by changes in CTD-derived **(a)** temperature (degrees Celsius), **(b)** salinity (practical salinity unit – psu), **(c)** oxygen saturation (percent) and **(d)** pH_T (total scale) depth profiles. Note that dips in salinity at the surface correspond with El-Niño-related torrential rain events further inland and a increased discharge of freshwater by the nearby river Rímac.

nitrate ammonification, i.e. dissimilatory nitrate or nitrite reduction to ammonium (DNRA), also leading to $^{30}N_2$ production via anammox (compare Fig. 1 and Holtappels et al., 2011). Incubations were in 12 mL glass double wadded exetainers (Labco Ltd.) in duplicates for each of the four time points, i.e. 0, ∼2, ∼7 and ∼20 h after label addition (in order to avoid potential bottle effects), in the dark, and inverted at a fairly constant 17±0.2 °C, close to respective in situ conditions (similar to the protocols described in Dalsgaard et al. (2003), Ward et al. (2009), and Bourbonnais et al. (2021)). All sample handling, such as filling of the exetainers with 8 mL of labelled sample water using an Eppendorf Multipette E3, was carried out in a glove box that had been evacuated three times with a vacuum pump, followed by flushing with N_2 4.5 gas (this was also done to the open exetainers). To reduce large background $^{28}N_2$ levels and facilitate the detection of the small isotopic signal of labelled N_2 being produced during incubations, the exetainers were capped and sparged with Helium 5.0 at 3 psi for 6 min on a manifold that could hold all 16 exetainers of a single mesocosm. Based on previous calculations and measurements, such a set-up will replace about 20 times the volume of each exetainer (unpublished data). This is lower than the 24 times reported to ensure that the reduction in O_2 concentration is by less than 20 % compared to in situ conditions (Holtappels et al., 2011). A similar reduction would also be observed for most other gases (Wanninkhof, 1992), except those buffered by conjugate acid–base pairs, such as H_2S or CO_2, for which the reduction would have been even less. Incubations were stopped at each time point by the injection of 50 µL of a $ZnCl_2$ solution (50 % w/v), followed by thorough mixing.

Exetainer vials were stored upside down at room temperature in the dark. Prior to analysis, the headspace and water were equilibrated at room temperature by placing the exetainers on a platform mixer at 100 rpm (revolutions per minute) overnight. For measurements, 100 µL of headspace from each exetainer was injected, using an autosampler (Carvalho and Murray, 2018), into a PLOT (porous layer open tubular) gas chromatography (GC) column, at 2 mL min^{-1}, housed in a TRACE GC oven and interfaced with a Thermo Scientific DELTA V Plus mass spectrometer via a GC Combustion III unit, followed by a liquid nitrogen trap. The latter

minimises interference by CO (a constituent in air) and NO (a secondary product during ionisation of water and/or oxygen, followed by the production of reactive oxygen species and recombination with nitrogen) due to imperfect GC column peak separation. The mass spectrometer was calibrated for N_2 concentrations by injections of known amounts of air.

Rate calculations were straightforward, as in most $^{15}NH_4^+$ incubations no enrichment over time in $^{29}N_2$ was detected, indicating the absence of anammox. Hence, denitrification in the $^{15}NO_2^-$ incubations (and because $^{30}N_2$ was quite noisy) was calculated from the increase in $^{29}N_2$ and the known ratio of labelled to unlabelled NO_2^- (in the rare cases where anammox was detected in the $^{15}NH_4^+$ incubations, denitrification was corrected for by subtraction). Rates were calculated from the linear regression slopes (see Fig. S1 in the Supplement) of the increase in the overall amount of N removed (as measured by areas ^{28}A and ^{29}A and associated $\delta^{15}N$), which was determined by the following conversions (modified from Thamdrup et al., 2006; Holtappels et al., 2011):

$$\begin{aligned} &N_{\text{removal}\,t1-3}\left(\mu\text{mol}\,N_2\,L^{-1}\right) \\ &\quad=\left[\left({}^{15}r\,\frac{\left({}^{28}A+{}^{29}A\right)\,c\,f_{\text{MS}}\,\frac{V_\text{h}}{V_\text{a}}}{f_{N_{2\text{air}}}\,c\,f_{{}^{15}N}}\right)_{t1-3}\right. \\ &\quad\left.-\left({}^{15}r\,\frac{\left({}^{28}A+{}^{29}A\right)\,c\,f_{\text{MS}}\,\frac{V_\text{h}}{V_\text{a}}}{f_{N_{2\text{air}}}\,c\,f_{{}^{15}N}}\right)_{t0}\right]\frac{1000}{V_\text{i}}, \end{aligned} \tag{1}$$

with

$${}^{15}r=\frac{{}^{15}R}{1+{}^{15}R}, \tag{2}$$

and

$${}^{15}R=\frac{\delta^{15}N}{1000}\,{}^{15}R_{\text{air}}+1, \tag{3}$$

where ^{15}R and $^{15}R_{\text{air}}$ denote the ratios of $^{15}N/^{14}N$ in a sample gas or air, respectively (the latter was determined from measured $^{28}N_2$ and $^{29}N_2$ by Junk and Svec, 1958, i.e. 0.00367647, and recommended by Coplen et al., 2002). $\delta^{15}N$ is the resulting isotopic composition (‰), V_h, V_i, and V_a are the volumes of headspace, sample incubated, and analysed (millilitres), respectively. $c\,f_{\text{MS}}$ is the determined calibration factor for each measurement run to convert mass spectrometer peak area ($^{28}A+^{29}A$) into abundance (µmol), $f_{N_{2\text{air}}}$ is the fraction of N_2 found in equilibrium in the 4 mL of headspace (V_h) in relation to the total amount, including the 8 mL of sample water (V_i), in an Exetainer, and $t1$–3 or $t0$ refer to the respective incubation sampling times. The conversion factor $f_{N2\text{air}}$ was calculated from N_2 solubility (Hamme and Emerson, 2004) for a lab temperature of 21 °C and a salinity of 35. To extrapolate from measured removal of ^{15}N to total N a conversion factor, $c\,f_{{}^{15}N}$ was calculated, taking into account the availability of labelled and overall substrate(s) together with the likelihood of $^{29}N_2$ production, i.e. $2F_N(1-F_N)$, for denitrification incubations (binomial), and F_N, for anammox, with F_N denoting the ratio of labelled to total $[NO_2^-]$ or $[NH_4^+]$, respectively.

It is noted that there have been studies which found discrepancies between denitrification calculated using $^{29}N_2$ as above, and $^{30}N_2$, due to non-binomial distributions (De Brabandere et al., 2014; Chang et al., 2014). This has been attributed to so-called intracellular NO_3^- / NO_2^- shunting, which leads to an error in the calculations of labelled to unlabelled substrate, based on known additions and measured seawater concentrations. With respect to noisy $^{30}N_2$ data, we cannot check if that was an issue here; yet, it would lead to an underestimation of denitrification rates in both cases. Given the good agreement between our rate measurements and a full nitrogen budget (see Sect. 3.2 for details), it, however, appears that potential NO_3^- / NO_2^- shunting did not affect our rate measurements significantly.

2.4 In situ substrate limitation of denitrification, total N loss calculations, and orni-eutrophication

In more than half of the denitrification incubations, measured N loss over a period of about 20 h was higher than the combined concentrations of in situ NO_3^- and NO_2^-. This indicates that the 3 µmol L^{-1} addition of $Na^{15}NO_2$ alleviated substrate limitation, and rates in the incubations were higher than theoretically sustainable at in situ conditions. Furthermore, acknowledging that rate measurements at different substrate concentrations in comparison to in situ conditions are always potential rates, we estimated in situ rates from a Michaelis–Menten kinetic by first calculating the maximum rate, $V_{\max}$, as follows:

$$V_{\max}=\frac{\text{Rate}_{\text{meas.}}\left([S]_{\text{in situ}}+\left[{}^{15}NO_2^-\right]+K_{1/2}\right)}{[S]_{\text{in situ}}+\left[{}^{15}NO_2^-\right]}, \tag{4}$$

which was followed by the realised rates at in situ substrate concentrations:

$$\text{Rate}_{\text{in situ}}=\frac{[S]_{\text{in situ}}\,V_{\max}}{[S]_{\text{in situ}}+K_{1/2}}, \tag{5}$$

with $[S]_{\text{in situ}}$ referring to in situ substrate concentrations of NO_2^- and NO_3^-, $[^{15}NO_2^-]$ referring to the 3 µmol L^{-1} label addition, and $K_{1/2}$ referring to the reaction half-saturation constant. As we have not performed any substrate vs. rate essays ourselves, and since there is only little information on the kinetics of water column denitrification, we adopted a conservative approach and chose the highest published $K_{1/2}$ of 5 µmol L^{-1} (Michiels et al., 2019), over the 2.9 and 2.5 µmol L^{-1} of Jensen et al. (2009) and Dalsgaard et al. (2013), respectively.

Total N loss by denitrification and anammox was calculated only for the first 38 d of the experiment. The reason was to keep the estimates by rate measurements comparable to estimates from a full N budget of the mesocosms,

as, after day 40, massive perturbations in the latter became obvious. This was caused by birds aggregating on the roofs of the mesocosms and depositing nitrogen-rich faeces (ornieutrophication). The onset of this perturbation was estimated by the sudden increase in total particulate phosphorus deposition rates in the sediment traps, most likely from excrement, as phosphate concentrations during this time were relatively constant (Fig. S2; for details see Bach et al., 2020a). Total N loss was then estimated by summing up hourly in situ rate estimates (Eq. 5) for each mesocosm (in case anammox was also detected, the measured rate was added to that of denitrification), factoring in the varying measurement intervals and, thus, filling in days without measurements. This hourly N_2 loss was then multiplied by $24\,\mathrm{h\,d^{1-}} \times 2$ (conversion between N_2 to N) and divided by three (average contribution of bottom layer water to overall mesocosm volume), converting it to total N loss over the first 38 d of the experiment.

2.5 Ancillary measurement parameters

Dissolved inorganic nutrient concentrations in seawater, i.e. NO_3^-, NO_2^-, and NH_4^+ (together referred to as DIN) and PO_4^{3-} and $Si(OH)_4$ were measured colourimetrically on a segmented flow analyser (QuAAtro, SEAL Analytical) on site (for details, see Bach et al., 2020a).

Dissolved organic nitrogen (DON) was calculated from a mass balance by subtracting measured DIN from total dissolved nitrogen (TDN) concentrations. The latter was also determined by segmented flow analysis after an oxidising step with Oxisolv (Merck) for 30 min in an autoclave.

Particulate organic nitrogen and carbon (PON and POC, respectively) concentrations in the water column were determined by filtering known amounts of seawater over precombusted glass fibre filters (GF/Fs) that were stored frozen until analysis on an elemental analyser (EA; EuroVector EA 3000; for details, see Bach et al., 2020a).

The removal of nitrogen from the water column via sedimentation (N_{sed}) was determined on material collected every other day from the sediment traps which was quantitatively precipitated, freeze-dried, weighed, and then an aliquot was measured on an elemental analyser (EuroVector EA 3000; for details, see Bach et al., 2020a and Boxhammer et al., 2016 again).

2.6 Statistical analyses

In order to assess what drives denitrification rates, stepwise multiple linear regressions (MLRs) with interaction terms were carried out. Prior to the regressions, outliers in estimated in situ denitrification rates (see Sect. 2.4 and Table 2 for details) were identified in a box-and-whisker plot and removed, i.e. five values with rates higher than $10\,\mathrm{nmol\,L^{-1}\,h^{-1}}$. In order to avoid overfitting and find a balance between model complexity and explanatory power, we followed a backward elimination process, starting with the full seven potential measured predictors, i.e. PON, PON_{sed}, DON, NO_3^-, NO_2^-, O_2, and H_2S, all measured in the bottom layer of the mesocosms (with the exception of sedimenting PON_{sed}). Note that we have opted to not include POC, which is highly co-correlated with PON, and DOC, which was not measured in the bottom layer (but probably would have a similar issue). In a next step, MLRs with all possible combinations of six potential predictors out of the overall seven and their resulting R^2 were calculated, which was followed by further MLRs, subsequently reducing the number of predictors each time by one (a total of 119 MLRs were fitted). Calculations were performed using the functions "boxplot", "stepwisefit", and "plotEffects" in MATLAB.

3 Results

The experiment took place during the 2017 coastal El Niño, which was characterised by three significant surface ocean warming events throughout January to April (Garreaud, 2018), with the last two, at the end of February and mid-March, clearly evident by the water surface temperatures above 22° C at our mooring site (Fig. 2a). The El Niño was accompanied by torrential rains further inland, which was reflected by periods of significant reductions in surface ocean salinity (Fig. 2b), coinciding with water discharge of more than twice the typical rates of the nearby river Rímac (Fig. S3). During our experiments, there were, however, also periods of deep water upwelling, as evidenced by colder surface ocean temperatures, and reduced oxygen saturation states and pH levels reaching down to ∼ 30 % and 7.5 (total scale), respectively (Fig. 2c, d).

3.1 Temporal changes in oxygen, inorganic nitrogen, and organic nitrogen, as well as hydrogen sulfide, in the bottom layer of the mesocosms

Thermal stratification of the Pacific Ocean and the mesocosm waters during the initial phase of the experiment meant strict separation of well-oxygenated surface (∼ 0–10 m) from oxygen-depleted bottom waters (Fig. 2c). And while in the surrounding Pacific bottom waters oxygen remained depleted throughout, corresponding oxygen levels in the mesocosms started to increase (Figs. 2 and 3e). This was caused by the cooling of the surface waters due to upwelling in the surrounding Pacific and the resultant mixing of surface and bottom waters in the mesocosms. Such artificial behaviour was mitigated by increasing bottom layer salinity and, therefore, stratification on days 13 and 33, which brought oxygen concentrations at depth down to typical Pacific levels again (Fig. 3e).

All mesocosms started with significant amounts of dissolved inorganic nitrogen present as NO_3^- and NO_2^-, which, however, were quickly depleted within the first 2 weeks (Fig. 3c, d). The deep water addition significantly increased

Table 2. Calculated in situ denitrification rates (nanomole dinotrogen per litre per hour; hereafter nmol N_2 L^{-1} h^{-1}) in the low N / P and very low N / P deep water addition mesocosms and the surrounding Pacific (see Sect. 2.4 for details), together with those for anaerobic ammonium oxidation (*anammox**) (nmol N_2 L^{-1} h^{-1}), when encountered, at various days. N loss refers to the total amount of nitrogen (micromole nitrogen per litre; hereafter µmol N L^{-1}) being lost through these processes for the first 38 d, for which an N budget can be calculated (compare Fig. 4). N loss was calculated for each mesocosm until day 38 by taking into account the varying measurement intervals and assuming an average contribution of bottom water to the overall mesocosm volume of one-third. For details on calculations, see Sect. 2. Note: SD – standard deviation. Note: anammox rates in the table below are shown in italics and with an asterisk to distinguish them from denitrification rates.

Mesocosm	In situ denitrification rates and/or *anammox** (nmol N_2 L^{-1} h^{-1})										N loss (µmol N L^{-1})	N budget (µmol N L^{-1})
Low N / P	*T*8	*T*12	*T*16	*T*22	*T*26	*T*30	*T*34	*T*38	*T*42	*T*46	*T*1–38	*T*1–38
M2	12.45	6.33	1.35	1.21	0.65	1.50	0.44	0.40	0.52	0.20	−2.39	−5.55
M3	4.29	9.52	7.90	6.62	2.06	0.57	0.74	5.79	1.67	0.21	−2.89	−3.38
M6	3.26	17.01	2.16	2.75	0.59	0.35	0.26	0.26	0.16	0.06	−2.00	−4.46
M7	4.89	3.62 *0.44**	2.43	0.23	0.48	0.38	0.00	0.17	0.17	0.15	−1.10	−3.00
Treatment mean ± SD											−2.10 ± 0.76	−4.10 ± 1.15
Very low N / P	*T*8	*T*12	*T*16	*T*22	*T*26	*T*30	*T*34	*T*38	*T*42	*T*46	*T*1–38	*T*1–38
M1	6.04	14.46	7.77	1.67	0.50	1.55	3.80	0.03	0.32	0.52	−2.73	−3.44
M4	0.66	32.71	7.26	4.81	7.58	4.19	0.10	0.08	0.04	0.01	−3.87	−7.23
M5	4.67	60.92	2.11	0.73	0.51	0.18	0.44	0.23	0.22	0.07	−4.79	−1.20
M8	9.13	5.77 *0.46**	1.88	0.34	0.25	0.45	0.23	0.15	0.15	0.02	−1.76	−0.87
Treatment mean ± SD											−3.29 ± 1.32	−3.19 ± 2.93
Overall mean ± SD											−2.69 ± 1.18	−3.64 ± 2.12
Pacific	8.32 *7.48**	1.96 *0.16**	5.94	17.27	0.09	2.67	0.21	0.00 *1.30**	0.25	48.46 *1.12**	−4.47	

NO_2^- concentrations in the low N / P treatments, although it made only a minor contribution to the overall nitrogen budget (see the following sections for details).

Initial particulate and dissolved organic nitrogen concentrations (PON and DON) at depth were similar in all mesocosms (between 6 and 10 µmol L^{-1}), and while there was no clear temporal trend for PON, DON saw a steady decline by about 30 % until day 40 (Fig. 3a, b).

H_2S concentrations at depth were in the micromolar range in all mesocosms and the surrounding Pacific and mostly oscillated between 3 and 10 µmol L^{-1} (Fig. 3f), equivalent to 0.1–0.3 ppm. In contrast, concentrations in surface waters were mostly in the high to low nanomolar range (data not shown).

3.2 Rates of denitrification and anammox and overall nitrogen loss

Measured denitrification rates in the 24 h incubations were similar in all mesocosms, ranging between less than 1 to up to ∼ 80 nmol L^{-1} h^{-1} (Table S1). More importantly, however, towards the end, measured rates exceeded those theoretically sustainable by substrate availability, i.e. combined in situ NO_3^- and NO_2^- concentrations. In comparison, measured denitrification rates in samples from the surrounding Pacific were comparable, although more variable, between consecutive measurement days.

Estimates for in situ denitrification (Eq. 5) were similar to measured rates at the beginning of the experiment when substrate availability was higher than or close to the half-saturation constant for denitrification. Towards the end, at high to low nanomolar substrate concentrations, in situ estimates were significantly lower (compare Tables 2 and S1).

Anammox was only detected on day 12 in mesocosms 7 and 8 at rates significantly smaller than those typical for denitrification (Table 2). In contrast, anammox was occasionally detected in the surrounding Pacific Ocean, i.e. on days 8, 12, and 46.

When comparing potential nitrogen loss, calculated as the sum of in situ estimates of denitrification and anammox over the first 38 d prior to the onset of orni-eutrophication (see Sect. 2.4 and Table 2 for details), with estimates of total nitrogen losses in each mesocosm from a nitrogen budget approach (compare Table 2 and Fig. 4 and see the next section for details), they were similar, with a mean of 2.69 ± 1.18 and 3.64 ± 2.12 µmol L^{-1}, respectively. It is acknowledged,

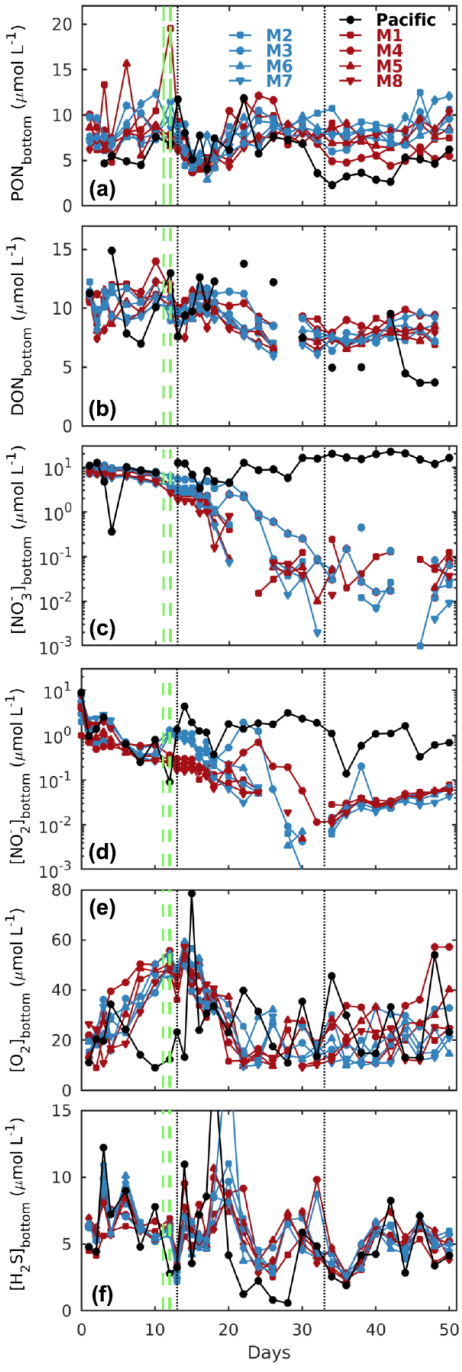

Figure 3. Temporal evolution of depth-integrated bottom layer **(a)** PON, **(b)** DON, **(c)** nitrate (NO_3^-), and **(d)** nitrite (NO_2^-), together with CTD-derived **(e)** oxygen (O_2) and **(f)** hydrogen sulfide (H_2S) concentrations at the Niskin sampling depth in the mesocosms (M1–M8) and the surrounding Pacific. Blue and red denote the low N / P and very low N / P deep water additions, respectively (see Sect. 2.2 for details). The dashed green lines denote deep water additions on days 11 and 12, while the dotted black lines denote additions of a brine solution to the bottom layer to increase salinity, strengthen stratification, and reduce mixing. See Sect. 2 for details.

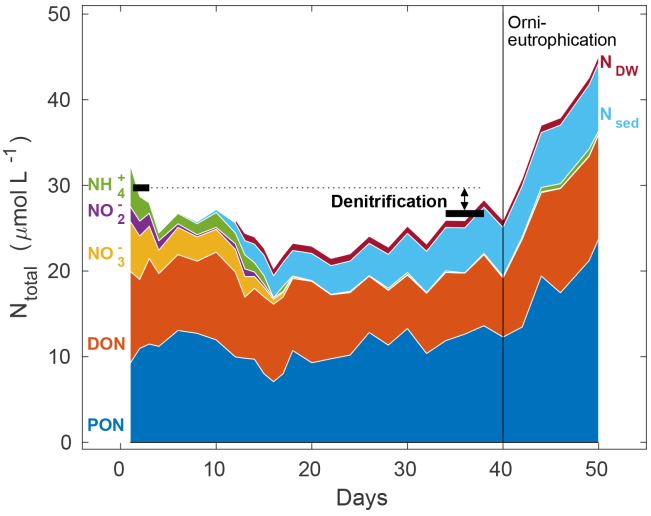

Figure 4. Representative example of a total nitrogen budget from mesocosm 7, considering all relevant pools such as particulate organic nitrogen (PON), dissolved organic nitrogen (DON), and dissolved inorganic nitrogen in the form of nitrate (NO_3^-), nitrite (NO_2^-), and ammonium (NH_4^+), cumulative particulate organic nitrogen exported to the sediment trap (N_{sed}), and the net change to all the above-mentioned nitrogen species (with the exception of PON, for which there was no deep water data) by deep water addition (N_{DW}). Black horizontal markers denote the total amount of nitrogen in these pools, calculated as an average of 3 consecutive sampling days at the start of the experiment (days 1–3) and towards the end (days 36–40), prior to the onset of orni-eutrophication. The deficit in this N budget comprises all nitrogen loss processes, dominated by denitrification (compare Table 2). Please note that the initial dip in nitrogen inventory is probably the result of a lag phase of nitrogen settling into the sediment trap.

however, that there was no statistically significant correlation between the two approaches.

3.3 Nitrogen budget

Summing up all organic and inorganic nitrogen species (excluding dissolved gases) in the water column, i.e. PON, DON, NO_3^-, NO_2^-, NH_4^+, N_{sed} (nitrogen exported through the sediment traps), and N_{DW} (overall deep water addition changes to the various nitrogen pools), revealed a first phase in all mesocosms for which the budget did not seem to be closed, as evidenced by a constant decline in total N during the first 2 weeks (Fig. 4). This was followed by a steady increase in total N until day 40, which was still below starting levels in all mesocosms. This net loss reflects, as we will argue below, the combined nitrogen loss processes, such as denitrification and anammox, exceeding nitrogen fixation, which was less than 0.1 µmol L^{-1} over the entire water column in this period (Leila Kittu, personal communication, 2020). Finally, the last 10 d were characterised by a rapid increase in total N, mostly driven by rising surface PON

concentrations, following continuous biomass production fuelled by external orni-eutrophication, i.e. the introduction of nitrogen-rich bird faeces to the mesocosms (see Bach et al., 2020a, for details).

3.4 Stepwise multiple linear regressions

In terms of R^2, there was a turning point in the number of potential main variables to explain in situ denitrification rates in stepwise multiple linear regressions (MLRs) with interactions. Above four to five independent variables, R^2 only increased slightly, while below it decreased relatively quickly (Fig. 5a). Both models with the highest R^2, for four and five main variables, identified NO_2^-, NO_3^-, and PON as those with the highest positive main effect sizes, with the remaining variables having relatively low effect sizes (Fig. 5b, d; Table 3). Finally, O_2 had a small negative main effect size in both models.

The resulting linear regression of in situ (compare Table 2) versus predicted denitrification rates slightly deviated from an ideal 1 : 1 relationship and had a small, yet positive, y axis intercept, meaning that lower denitrification rates would be over, while higher ones underestimated (Fig. 5c).

4 Discussion

A discussion on the unusual situation of a coastal El Niño during our study period, i.e. significant warming of surface waters, increasing stratification, and reducing upwelling intensity and/or frequency can be found elsewhere (Bach et al., 2020a). Most importantly, however, there were also multiple upwelling events in the surrounding Pacific during this time which were of similar magnitude to our experimental upwelling (Chen et al., 2021), providing the natural context.

4.1 Denitrification rates and nitrogen budgets

Denitrification rates measured in the incubations of water from the mesocosms and the surrounding Pacific of up to $\sim 80\,\mathrm{nmol\,N_2\,L^{-1}\,h^{-1}}$ (although mostly well below, at a median of 12.4) were within the range of reported rates in Peruvian ODZ and OMZ waters (Farías et al., 2009; Dalsgaard et al., 2012). This was despite significantly higher oxygen concentrations here than typical for suboxic ODZs, i.e. less than $\sim 6\,\mu\mathrm{mol\,L^{-1}}$ (Tyson and Pearson, 1991; Yang et al., 2017), although denitrification can be relatively insensitive to oxygen concentrations of up to at least 30–40 $\mu\mathrm{mol\,L^{-1}}$ (Farías et al., 2009), which is higher than levels in our study for most of the time (see Fig. 3 but also Sect. 4.2.2).

Most interestingly, measured denitrification rates in incubations of mesocosm waters during the second half of the experiment exceeded those theoretically sustainable at in situ substrate availability (compare Sect. 2.4 and Table 2). Nitrification, supplying additional nitrite for denitrification, can operate at low micromolar (and even nanomolar) levels such as those found in our study (Bristow et al., 2016). However, a significant contribution to measured denitrification rates is unlikely as there and elsewhere (Peng et al., 2016; Santoro et al., 2021) nitrification rates were usually at least an order of magnitude lower than our measured denitrification rates. Hence, the reason for higher measured rates is most likely found in the fact that both NO_3^- and NO_2^- concentrations had dropped below 0.1 or even 0.01 $\mu\mathrm{mol\,L^{-1}}$ during this stage, indicating that the denitrifying community was actually substrate limited. Such an observation was also made by Michiels et al. (2019) in a temperate fjord system. In comparison, denitrification rates in the surrounding Pacific waters had a higher day-to-day variability, and substrate limitation only occurred once. This is to be expected in a much more variable system characterised by frequent upwelling events of oxygen-depleted waters (Fig. 2) with relatively higher NO_3^- and NO_2^- concentrations (Fig. 3c, d).

Calculated Michaelis–Menten kinetic scaled estimates for in situ denitrification in the mesocosms and the surrounding Pacific were lower than measured rates during the incubations. This was particularly the case during the second half of the experiment, which reinforces the notion of substrate limitation.

The primary drivers of in situ denitrification rates appeared to be the availability of NO_2^- and NO_3^-, followed by particulate organic matter (nitrogen), as indicated by multiple linear regression and effect size analysis (Fig. 5). This suggests that heterotrophic rather than chemolithotrophic denitrification was dominant (compare Sect. 4.2.2), as all three are substrates for the former process and eventually limit rates. The reason for NO_2^- rather than NO_3^- concentrations explaining the rates of denitrification in one of the MLRs could be found in the following. As denitrification from NO_3^- to N_2 involves multiple and independent steps and organisms, the correlation between the N_2 production rate and a substrate concentration should become better the closer one comes to the end of this chain (Fig. 1). For example, there should be a perfect correlation between N_2O concentrations and N_2 production rate, and NO_3^- concentrations and their turnover to NO_2^- are meaningless if the intermediate steps to nitric and nitrous oxide are blocked or constitute a bottleneck. This would also contribute to the finding that denitrification rate measurements based on $^{15}NO_3^-$ can be lower than those based on $^{15}NO_2^-$ (Hamersley et al., 2007).

Overall nitrogen loss, calculated from in situ denitrification rates over the first 38 d of the experiment prior to the onset of orni-eutrophication, was comparable to an alternative estimate that was based on a full nitrogen budget in each mesocosm (Fig. 4; Table 2). The means of both methods, i.e. 2.69 ± 1.18 and 3.64 ± 2.12, were insignificantly different, although there was no statistically significant correlation when all mesocosms were compared. However, given that the nitrogen budget calculations involved a mass balance of seven entities with individual measurement uncertainties, this probably does not come as a surprise. There were also

Table 3. Multiple linear regression statistics (standard error – SE; t and p values), describing denitrification in response to various environmental variables, for the best five-variable model (in terms of R^2), with interactions (compare Fig. 5c), and the best four-variable model.

	Estimate	SE	t	p		Estimate	SE	t	p
(Intercept)	2.5529	1.5437	1.6537	0.104	(Intercept)	0.7507	1.0888	0.6894	0.4933
PON	0.0039	0.1037	0.0377	0.970	PON	−0.0382	0.1118	−0.3420	0.734
NO_3^-	3.2562	1.1318	2.8770	0.006	NO_3^-	5.9709	0.7551	7.9072	< 0.001
NO_2^-	−5.1120	9.3374	−0.5475	0.586	NO_2^-	−29.494	4.8048	−6.1385	< 0.001
O_2	−0.0964	0.0515	−1.8742	0.066	O_2	4.72×10^{-4}	0.0234	0.0202	0.984
H_2S	−0.4238	0.2360	−1.7958	0.078	PON / NO_3^-	−0.3501	0.0624	−5.6093	< 0.001
PON / NO_3^-	−0.3568	0.0593	−6.0169	< 0.001	PON / NO_2^-	4.3858	0.6737	6.5103	< 0.001
PON / NO_2^-	3.7572	0.6650	5.6499	< 0.001	NO_3^- / NO_2^-	−3.5869	0.8114	−4.4207	< 0.001
NO_3^- / NO_2^-	−2.4176	0.6895	−3.5065	< 0.001	NO_3^- / O_2	−0.0434	0.0122	−3.5715	< 0.001
NO_3^- / O_2	−0.0350	0.0107	−3.2777	0.002	NO_3^- / O_2	0.1829	0.0570	3.2073	0.002
NO_3^- / H_2S	0.3773	0.1476	2.5571	0.013					
NO_2^- / H_2S	−2.5429	0.8945	−2.8429	0.006					
O_2 / H_2S	0.0183	0.0090	2.0350	0.047					
R^2				0.8109	R^2				0.7666

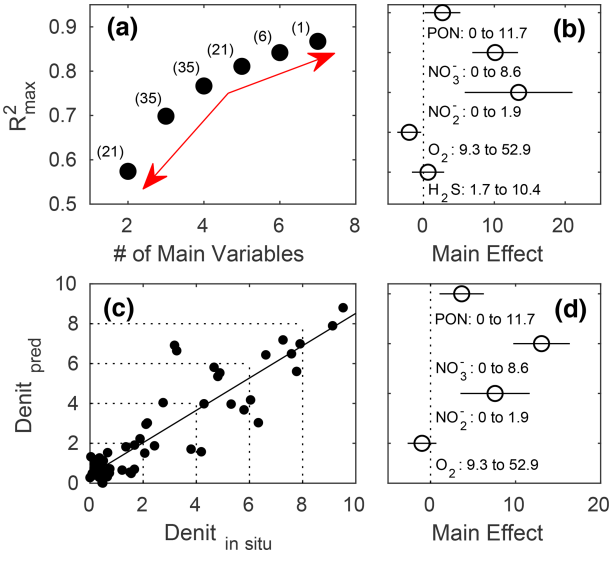

Figure 5. Stepwise multiple linear regressions (MLRs) of in situ denitrification rates in the mesocosms against up to seven potential predictors and their interactions (PON, PON_{sed}, DON, NO_3^-, NO_2^-, O_2, and H_2S), with the **(a)** reducing numbers of measured variables and resulting maximum R^2. The red arrows denote the relatively small increase in maximum R^2 beyond five main variables and the relatively large decrease below, indicating this to be the sweet spot in terms of balancing the model complexity with predictive power and avoiding overfitting (see Sect. 2 for details). Numbers in parentheses denote the number of possible predictor combinations, i.e. MLRs fitted. **(b)** Main effect sizes of the stepwise MLRs with five main variables and the highest (0.8109) R^2 (compare Table 3). **(c)** Linear fit through in situ and predicted denitrification rates (nanomole dinitrogen per litre per hour; hereafter nmol N_2 L^{-1} h^{-1}) by the MLR with five main variables. **(d)** Main effect sizes of the stepwise MLR with four main variables and the highest (0.7666) R^2 (compare Table 3).

no statistically significant differences between the two deep water addition treatments, which was most likely due to relatively small differences in dissolved inorganic nitrogen in both waters in relation to the overall nitrogen pool in the mesocosms and a similar N deficit in both deep water batches (Table 1). However, N loss estimated from in situ denitrification rates in the low N / P mesocosms was significantly lower than the budget estimate. It is noted, however, that in situ denitrification rates are a conservative estimate that potentially underestimate the true loss. For instance, adopting a lower half-saturation rate constant of 2 µmol L^{-1} (Eqs. 4 and 5) would remove any statistically significant difference between the two approaches. Furthermore, NO_3^- and NO_2^- standing stocks most likely underestimate availability and, hence, in situ denitrification rates calculated here because of hidden turnover.

Finally, modelling exercises suggest that nitrogen loss in the water column is linked with mature El Niño/La Niña periods, with up to 70 % reduced rates during the former, most likely linked to increased water column oxygen concentrations at reduced upwelling and/or enhanced stratification (Deutsch et al., 2011; Yang et al., 2017), and increasing mesoscale turbulence and associated offshore nutrient export by eddies (Espinoza-Morriberón et al., 2017). This suggests that the rates observed here could actually be significantly higher in the more frequent La Niña periods.

4.2 Rates of anammox and the lack thereof in the mesocosms

Anammox and denitrification were first reported in the eastern tropical South Pacific (ETSP) in 2006 (Thamdrup et al., 2006), and the ETSP remains the most frequently sampled and most thoroughly characterised open ocean OMZ region. Anammox was the dominant N loss process in several stud-

ies, where denitrification was either not (Hamersley et al., 2007) or only sporadically (Kalvelage et al., 2013) detected. Subsequent studies in the ETSP detected both processes, and anammox was a substantial and mostly dominant part of the total N loss. There was an average of 78 % anammox along a Chilean coastal transect (Dalsgaard et al., 2012), 82 %–90 % at two high-resolution stations (De Brabandere et al., 2014), and 49 ± 20 % over four high-resolution stations (Babbin et al., 2020).

Anammox requires a source of NH_4^+ and NO_2^-, which must either be produced in situ by the remineralisation of organic matter in the absence of oxygen (as, for instance, by denitrification) or must be transported into the system from elsewhere, e.g. from adjacent sediments (Ward, 2013). When both processes are supported by organic matter remineralisation, then there is theoretical (Paulmier et al., 2009; Koeve and Kähler, 2010) and experimental evidence (Babbin et al., 2014) that the ratio of denitrification to anammox should be connected to the elemental composition of organic matter being decomposed, at least on larger spatial and temporal scales. The reasoning behind this connection is that complete anaerobic organic matter decomposition by denitrification produces NH_4^+ and N_2 in quantities mostly dependent on the carbon to nitrogen ratio (C / N) of the organic matter being decomposed. Hence, this ratio dictates the denitrification (only utilising NO_3^- and/or NO_2^-) to anammox (utilising both NO_2^- and NH_4^+) ratio in a steady state (Babbin et al., 2014). However, DNRA could also supply NH_4^+ for anammox. Although there have been reports of DNRA in the ETSP (Lam et al., 2009), it is usually negligible in the water column (De Brabandere et al., 2014; Kalvelage et al., 2013) and rather restricted to shallow coastal systems dominated by sediments (Jensen et al., 2011). In the absence of DNRA, complete anaerobic decomposition of average phytoplankton-derived organic matter, i.e. $C_{106}H_{175}O_{42}N_{16}P$ (Anderson, 1995), would require a ~ 28 % contribution of anammox to overall N loss via these two processes (Babbin et al., 2014).

The reason for an anammox dominance in several studies mentioned above, despite above outlined stoichiometric constraints, could be partial denitrification of NO_3^- to NO_2^- without the following steps leading to N_2 production, supplying both NO_2^- and NH_4^+ for anammox (Lam et al., 2009; Jensen et al., 2011; Kalvelage et al., 2013; Peters et al., 2016). Furthermore, the ratio of NO_2^- to NH_4^+ produced by organic matter decomposition of a certain C / N ratio could also be influenced by anaerobic chemolithotrophic nitrite oxidation (compare Fig. 1), looping NO_2^- back to NO_3^- for further partial denitrification and associated NH_4^+ production (Babbin et al., 2020).

In summary, anammox, in the absence of denitrification, is difficult to explain (although partial denitrification is not easily detected), while denitrification in the absences of anammox is rarely observed in the ETSP but presents no stoichiometric conflicts.

4.2.1 Organic matter C / N in mesocosms

For the first 38 d of the experiment, particulate organic matter in the bottom layer of the mesocosms, where the N loss process incubation samples were taken from, had a C / N of ~ 7–8 (compare Bach et al., 2020a), which would not change the theoretical anammox contribution of ~ 28 % by much. However, this ratio could be misleading as the particulate organic matter will be comprised by more and less labile fractions. A good proxy for that should be to just consider the freshly produced organic matter, i.e. the particulate and dissolved matter in the sunlit surface layer of the mesocosms in our case. Interestingly, just looking at C / N of standing stocks for particulate organic matter, it was initially lower than in the bottom layer, indicative of preferential nitrogen remineralisation at depth, but increased to values of ~ 10 in all mesocosms but one (no bloom of the dinoflagellate *Akashiwo sanguinea*; see Bach et al. (2020a), for details) after the deep water addition (Fig. S4). Similarly, C / N in dissolved organic matter started already at about 10, increasing to up to 30 after the deep water addition, and when summed up to total organic matter, C / N levels of up to 20 were reached (Fig. S4). Increasing C / N from 6.625 to 20 would reduce the theoretical anammox contribution to only about 10 %. Furthermore, as already mentioned above, it should not be the standing stocks that are considered but the actual fresh production. Unfortunately, neither C nor N production were directly measured, but gauging the change in total organic carbon (TOC) concentrations after the deep water addition suggests that at least $\sim 100\,\mu mol\,L^{-1}$ were produced (Fig. S4). In contrast, total organic nitrogen (TON) concentrations hardly changed at all, suggesting even higher C / N in freshly produced organic matter than in measured standing stocks. This could be the result of general dissolved inorganic nitrogen limitation and, hence, carbon overconsumption (Toggweiler, 1993) but also changes in the phytoplankton community composition (see Bach et al., 2020a, for details). It is noted, though, that changes in organic matter standing stocks over time are not necessarily a good indicator of the quantity and quality of fresh production due to unknown and potentially different turnover times for each element, although it is probably better than using standing stocks themselves. In this sense, the ODZ/OMZ signature of upwelled water, i.e. its nitrogen deficit, should influence the ratio of denitrification to anammox that is subsequently measured. Hence, regions with either one or the other process dominating could be indicative of the upwelling source water history.

4.2.2 Oxygen and hydrogen sulfide in mesocosms

Varying ratios of anammox to denitrification could also be the result of different sensitivities of both processes to prevailing oxygen concentrations. However, while there are a few experiments that have directly addressed the oxygen sensitivity of various N cycling processes, there appears to

be no straightforward answer. For instance, in manipulative experiments, Jensen et al. (2008) found anammox at oxygen concentrations of up to $\sim 12.5\,\mu mol\,L^{-1}$, with denitrification not encountered at all. This is similar to Kalvelage et al. (2011), who observed anammox to cease above $\sim 20\,\mu mol\,L^{-1}$. And although no full denitrification was observed to at least N_2O or N_2O, the first step from NO_3^- to NO_2^- was found to occur even at the highest oxygen concentration of $\sim 25\,\mu mol\,L^{-1}$. This is, in turn, consistent with the nitrate reduction observed to at least N_2O at oxygen concentrations of up to ~ 30–$40\,\mu mol\,L^{-1}$ (Frey et al., 2020). In contrast, both anammox and denitrification can already be significantly or completely inhibited by oxygen additions of 3 or $8\,\mu mol\,L^{-1}$ (Babbin et al., 2014) or even lower (Dalsgaard et al., 2014). In essence, there is no clear indication of one process being more sensitive to oxygen than the other, which is potentially also related to variability in oxygen concentrations on small scales, i.e. in microenvironments around particles which are not captured by bulk seawater oxygen concentration measurements. And, indeed, there is evidence that microbial diversity in the OMZ is critically linked to particles, as are rates of denitrification and anammox (Ganesh et al., 2014, 2015).

The situation appears to be similar for H_2S, which, furthermore, has been observed to reach $10\,\mu mol\,L^{-1}$ and even higher in the coastal subsurface ETSP close to our study location (Callbeck et al., 2018, 2019). H_2S has been reported to completely inhibit anammox at $3\,\mu mol\,L^{-1}$ (Jensen et al., 2008), a concentration similar to that at the bottom layer of our mesocosms, while Dalsgaard et al. (2014) found no effect on N_2 production by anammox, or denitrification, at slightly lower levels of $1\,\mu mol\,L^{-1}$. Concerning denitrification, Dalsgaard et al. (2013) reported no effects of H_2S at even higher concentrations of up to $10\,\mu mol\,L^{-1}$, which is in the range of maximum concentrations found in our study, and there was stimulation in some instances, although this is most likely related to chemolithotrophic as opposed to heterotrophic denitrification (see Dalsgaard et al., 2013; Bonaglia et al., 2016, and references therein). Chemolithotrophic denitrification coupled to H_2S oxidation has also been hypothesised for coastal high H_2S stations off Peru by Kalvelage et al. (2013). Interestingly, by day 16 and onwards, the anammox functional marker gene hzo (Schmid et al., 2008) was not detectable anymore in any of the mesocosms (data not shown), which could be linked to relatively high H_2S concentrations, explaining the lack of anammox – at least for most parts of the experiment.

5 Conclusions: ODZ/OMZ nitrogen budget implications

The loss of, on average, 3–$4\,\mu mol\,L^{-1}$ of nitrogen in our mesocosms fits well to zonal estimates by DeVries et al. (2012) for the ODZ in the eastern South Pacific between 75–100 m depth, where oxygen levels were similar to those encountered in our study (Chang et al., 2010), although the latter study reported a 2–3 times higher nitrogen deficit. Furthermore, the overall amount of nitrogen loss measured in the Pacific was at the upper end of ranges encountered in the mesocosms, potentially connected to substrate limitation in the mesocosms during the second half of the experiment (Table 2).

In contrast to shipboard measurements, the mesocosms offer the unique opportunity to put the various nitrogen pathways, i.e. loss as opposed to initial bioavailable standing stocks and export, into context. Between ~ 1 and $5.5\,\mu mol\,L^{-1}$ of nitrogen were lost as N_2, representing up to 20 % of the initially bioavailable inorganic and organic nitrogen until day 38 of the experiment (compare Table 2 and Fig. 4). Interestingly, the amount of particulate organic nitrogen being exported below 20 m, i.e. the approximate depth of the sediment traps at the bottom of the mesocosms (compare Fig. 1 in Bach et al., 2020a), was in the same range. This indicates that, in the Peruvian EBUS, about half of the nitrogen that could be exported to depth would already be lost, i.e. converted to N_2, in a relatively shallow layer of the surface ocean, provided that there were oxygen-deficient conditions during the coastal upwelling as in our study (Fig. 2). Furthermore, over the entire pelagic water column, nitrogen loss of exported organic matter is likely to be even higher, suggesting that the majority of the dissolved inorganic nitrogen assimilated during new production (equalling export production on larger scales) should actually be lost in EBUSs.

Similar conclusions can also be reached by alternative means, i.e. by starting with global export production. Recent estimates based on observations and models range between ~ 5 and $15\,Pg\,C\,yr^{-1}$, also including, next to the gravitation-driven biological pump, those by particle injection (see Boyd et al., 2019, and references therein). Assuming a Redfield molar C / N of 6.625 (Redfield et al., 1963) would translate to 0.75–$2.26\,Pg\,N\,yr^{-1}$ being exported. Furthermore, considering that about 5 % of global primary production and, hence, potential export production is located in the surface ocean of the four major EBUSs (Carr, 2002), the Arabian Sea (Vijayaraghavan and Krishna Kumari, 1989) and the Bay of Bengal (Poornima et al., 2020) above the ODZs and OMZs, about 38–$113\,Tg\,N\,yr^{-1}$ could potentially be lost. In comparison, estimates of water column denitrification and/or anammox, i.e. 20 %–35 % of total marine losses of about $260 \pm 100\,Tg\,N\,yr^{-1}$ (see Zhang et al., 2020, and references therein), then range between 52 ± 20 and $91 \pm 35\,Tg\,N\,yr^{-1}$, indicating that a significant portion, if not the majority, of the exported nitrogen is indeed lost in ODZs and OMZs.

Nitrogen cycling in ODZs and OMZs currently plays a very important role in the overall marine nitrogen budget. However, the magnitude and direction of change in the actual nitrogen loss term in response to ongoing climate and ocean change (e.g. ocean stratification, acidification, and/or changes in temperature and oxygen levels) is uncertain. This

issue is further complicated by uncertainties in future primary productivity and organic matter export estimates. For instance, depending on the representative concentration pathway, future export production could decrease as a result of changes to community structure (see Bindoff et al., 2019, for details and references therein). In summary, future changes in upwelling intensity and frequency, as well as the other potential biotic and abiotic factors mentioned above, could change the nitrogen (im)balance in ODZs and OMZs, having a significant impact on the overall marine nitrogen budget.

Data availability. The majority of the data are available at https://doi.org/10.1594/PANGAEA.923395 (Bach et al., 2020b), with some additional data being presented in the tables in this paper.

Supplement. The supplement related to this article is available online at: https://doi.org/10.5194/bg-18-4305-2021-supplement.

Author contributions. KGS, LB, TB, AL, and UR designed the experiment. KGS, JA, LB, TB, MI, VK, AL, JaM, JuM, FM, EvdE, and UR contributed to the sampling and various measurements. DE helped with ^{15}N data interpretation, and BBW introduced KGS to denitrification and anammox assay incubations. All authors analysed the data, and KGS wrote the paper, with the co-authors contributing with comments on the content.

Competing interests. The authors declare that they have no conflict of interests.

Disclaimer. Publisher's note: Copernicus Publications remains neutral with regard to jurisdictional claims in published maps and institutional affiliations.

Special issue statement. This article is part of the special issue "Ecological and biogeochemical functioning of the coastal upwelling system off Peru: an in situ mesocosm study". It is not associated with a conference.

Acknowledgements. We thank all participants of the KOSMOS mesocosm study 2017 in the coastal upwelling system off Peru for assisting in mesocosm sampling and maintenance. We are particularly thankful to the staff of IMARPE for their support during the planning, preparation, and execution of this study and to the captains and crews of *BAP Morales*, *IMARPE VI* and *BIC Humboldt*, for their support during deployment and recovery of the mesocosms and various operations during the course of this investigation. Special thanks go to the Marina de Guerra del Peru, in particular to the submarine section of the navy of Callao and to the Dirección General de Capitanías y Guardacostas. We also acknowledge strong support, for the sampling and mesocosm maintenance, by Jean-Pierre Bednar, Gabriela Chavez, Susanne Feiersinger, Peter Fritsche, Paul Stange, Anna Schukat, and Michael Krudewig. We want to thank Club Náutico Del Centro Naval, for the excellent hosting of our temporary filtration laboratory, office space, and their great support and improvisation skills after two of our boats were lost. This work is a contribution in the framework of the Cooperation agreement between the IMARPE and GEOMAR through the German Ministry for Education and Research (BMBF; project no. ASLAEL 12-016) and the Integrated Study of the Upwelling System off Peru developed by the Direction of Oceanography and Climate Change of IMARPE (project no. PPR 137 CONCYTEC). Furthermore, the Servicio Nacional de Meteorología e Hidrología del Perú (SENAMHI) is thanked for providing the Rímac discharge data. Finally, Matheus Carvalho de Carvalho is thanked for the N_2 isotope measurements.

Financial support. This research has been supported by the Collaborative Research Center (SFB 754), "Climate–Biogeochemistry Interactions in the Tropical Ocean", financed by the German Research Foundation (DFG), the Leibniz Award 2012 (granted to Ulf Riebesell), the Helmholtz International Fellow Award 2015 (granted to Javier Arístegui), and EU funding by AQUACOSM (granted to a number of participants, including Javier Arístegui and Kai G. Schulz).

Review statement. This paper was edited by Hans-Peter Grossart and reviewed by Annie Bourbonnais and one anonymous referee.

References

Anderson, L. A.: On the hydrogen and oxygen content of marine phytoplankton, Deep-Sea Res. Pt. I, 42, 1675–1680, 1995.

Babbin, A. R., Keil, R. G., Devol, A. H., and Ward, B. B.: Organic Matter Stoichiometry, Flux, and Oxygen Control Nitrogen Loss in the Ocean, Science, 344, 406–408, 2014.

Babbin, A. R., Buchwald, C., Morel, F. M. M., Wankel, S. D., and Ward, B. B.: Nitrite oxidation exceeds reduction and fixed nitrogen loss in anoxic Pacific waters, Mar. Chem., 224, 103814, https://doi.org/10.1016/j.marchem.2020.103814, 2020.

Bach, L. T., Paul, A. J., Boxhammer, T., von der Esch, E., Graco, M., Schulz, K. G., Achterberg, E., Aguayo, P., Arístegui, J., Ayón, P., Baños, I., Bernales, A., Boegeholz, A. S., Chavez, F., Chavez, G., Chen, S.-M., Doering, K., Filella, A., Fischer, M., Grasse, P., Haunost, M., Hennke, J., Hernández-Hernández, N., Hopwood, M., Igarza, M., Kalter, V., Kittu, L., Kohnert, P., Ledesma, J., Lieberum, C., Lischka, S., Löscher, C., Ludwig, A., Mendoza, U., Meyer, J., Meyer, J., Minutolo, F., Ortiz Cortes, J., Piiparinen, J., Sforna, C., Spilling, K., Sanchez, S., Spisla, C., Sswat, M., Zavala Moreira, M., and Riebesell, U.: Factors controlling plankton community production, export flux, and particulate matter stoichiometry in the coastal upwelling system off Peru, Biogeosciences, 17, 4831–4852, https://doi.org/10.5194/bg-17-4831-2020, 2020a.

Bach, L. T., Paul, A. J., Boxhammer, T., von der Esch, E., Graco, M., Schulz, K. G., Achterberg, E., Aguayo, P., Aristegui, J., Ayon, P., Banos, I., Bernales, A., Boegeholz, A. S., Chavez,

F., Chen, S.-M., Doering, K., Filella, A., Fischer, M., Grasse, P., Haunost, M., Hennke, J., Hernandez-Hernandez, N., Hopwood, M., Igarza, M., Kalter, V., Kittu, L., Kohnert, P., Ledesma, J., Lieberum, C., Lischka, S., Loescher, C., Ludwig, A., Mendoza, U.,Meyer, J., Meyer, J., Minutolo, F., Ortiz Cortes, J., Piiparinen, J., Sforna, C., Spilling, K., Sanchez, S., Spisla, C., Sswat, M., Zavala Moreira, M., and Riebesell, U.: KOSMOS 2017 Peru mesocosm study: overview data, PANGAEA [Dataset], https://doi.org/10.1594/PANGAEA.923395, 2020b.

Bakun, A. and Weeks, S. J.: The marine ecosystem off Peru: What are the secrets of its fishery productivity and what might its future hold?, Progr. Oceanogr., 79, 290–299, 2008.

Bianchi, D., Dunne, J. P., Sarmiento, J. L., and Galbraith, E. D.: Data-based estimates of suboxia, denitrification, and N_2O production in the ocean and their sensitivities to dissolved O_2, Global Biogeochem. Cy., 26, GB2009, https://doi.org/10.1029/2011GB004209, 2012.

Bindoff, N. L., Cheung, W. W. L., Arístegui, J. G. K. J., Guinder, V. A., Hallberg, R., Hilmi, N., and Williamson, P.: Chapter 5: Changing ocean, marine ecosystems, and dependent communities, IPCC special report oceans and cryospheres in changing climate, Cambridge, University Press, 2019.

Bograd, S. J., Castro, C. G., Di Lorenzo, E., Palacios, D. M., Bailey, H., Gilly, W., and Chavez, F. P.: Oxygen declines and the shoaling of the hypoxic boundary in the California Current, Geophys. Res. Lett., 35, L12607, https://doi.org/10.1029/2008GL034185, 2008.

Bonaglia, S., Klawonn, I., De Brabandere, L., Deutsch, B., Thamdrup, B., and Brüchert, V.: Denitrification and DNRA at the Baltic Sea oxic–anoxic interface: Substrate spectrum and kinetics, Limnol. Oceanogr., 61, 1900–1915, 2016.

Bopp, L., Le Quéré, C., Heimann, M., Manning, A. C., and Monfray, P.: Climate-induced oceanic oxygen fluxes: Implications for the contemporary carbon budget, Global Biogeochem. Cy., 16, 1022, https://doi.org/10.1029/2001GB001445, 2002.

Bourbonnais, A., Letscher, R. T., Bange, H. W., Échevin, V., Larkum, J., Mohn, J., Yoshida, N., and Altabet, M. A.: N_2O production and consumption from stable isotopic and concentration data in the Peruvian coastal upwelling system, Global Biogeochem. Cy., 31, 678–698, 2017.

Bourbonnais, A., Frey, C., Sun, X., Bristow, L. A., Jayakumar, A., Ostrom, N. E., Casciotti, K. L., and Ward, B. B.: Protocols for Assessing Transformation Rates of Nitrous Oxide in the Water Column, Front. Mar. Sci., 8, 611937, https://doi.org/10.3389/fmars.2021.611937, 2021.

Boxhammer, T., Bach, L. T., Czerny, J., and Riebesell, U.: Technical note: Sampling and processing of mesocosm sediment trap material for quantitative biogeochemical analysis, Biogeosciences, 13, 2849–2858, https://doi.org/10.5194/bg-13-2849-2016, 2016.

Boyd, P. W., Claustre, H., Levy, M., Siegel, D. A., and Weber, T.: Multi-faceted particle pumps drive carbon sequestration in the ocean, Nature, 568, 327–335, 2019.

Brandes, J. A., Devol, A. H., and Deutsch, C.: New Developments in the Marine Nitrogen Cycle, Chem. Rev., 107, 577–589, 2007.

Bristow, L. A., Dalsgaard, T., Tiano, L., Mills, D. B., Bertagnolli, A. D., Wright, J. J., Hallam, S. J., Ulloa, O., Canfield, D. E., Revsbech, N. P., and Thamdrup, B.: Ammonium and nitrite oxidation at nanomolar oxygen concentrations in oxygen minimum zone waters, P. Natl. Acad. Sci. USA, 113, 10601–10606, 2016.

Bryan, J. R., Riley, J. P., and Williams, P. J. L.: A Winkler procedure for making precise measurements of oxygen con-centration for productivity and related studies, J. Exp. Mar. Biol. Ecol., 21, 191–197, 1976.

Brzezinski, M. A.: The Si:C:N Ratio of Marine Diatoms: Interspecific Variability and the Effect of some Environmental Variables, J. Phycol., 21, 347–357, 1985.

Callbeck, C., Lavik, G., Ferdelman, T. G., Fuchs, B., Gruber-Vodicka, H. R., Hach, P. F., Littmann, S., Schoffelen, N. J., Kalvelage, T., Thomsen, S., Schunck, H., Löscher, C. R., Schmitz, R. A., and Kuypers, M. M. M.: Oxygen minimum zone cryptic sulfur cycling sustained by offshore transport of key sulfur oxidizing bacteria, Nat. Commun., 9, 1729, https://doi.org/10.1038/s41467-018-04041-x, 2018.

Callbeck, C., Pelzer, C., Lavik, G., Ferdelman, T. G., Graf, J. S., Vekeman, B., Schunck, H., Littmann, S., Fuchs, B. M., Hach, P. F., Kalvelage, T., Schmitz, R. A., and Kuypers, M. M. M.: *Arcobacter peruensis* sp. nov., a chemolithoheterotroph isolated from sulfide-and organic-rich coastal waters off Peru, Appl. Environ. Microbiol., 85, e01344-19, https://doi.org/10.1128/AEM.01344-19, 2019.

Carr, M. E.: Estimation of potential productivity in Eastern Boundary Currents using remote sensing, Deep-Sea Res., 49, 59–80, 2002.

Carritt, D. E. and Carpenter, J. H.: Comparison and Evaluation of Currently Employed Modifications of the Winkler Method for Determining Dissolved Oxygen in Seawater; A NASCO Report, J. Mar Res., 24, 286–318, 1966.

Carvalho, M. C. and Murray, R. H.: Osmar, the open-source microsyringe autosampler, HardwareX, 3, 10–38, 2018.

Chang, B. X., Devol, A. H., and Emerson, S. R.: Denitrification and the nitrogen gas excess in the eastern tropical South Pacific oxygen deficient zone, Deep-Sea Res., 57, 1092–1101, 2010.

Chang, B. X., Rich, J. R., Jayakumar, A., Naik, H., Pratihary, A. K., Keil, R. G., Ward, B. B., and Devol, A. H.: The effect of organic carbon on fixed nitrogen loss in the eastern tropical South Pacific and Arabian Sea oxygen deficient zones, Limnol. Oceanogr., 59, 1267–1274, 2014.

Chavez, F. P. and Messié, M.: A comparison of Eastern Boundary Upwelling Ecosystems, Progr. Oceanogr., 83, 80–96, 2009.

Chen, S.-M., Riebesell, U., Schulz, K. G., von der Esch, E., Achterberg, E. P., and Bach, L. T.: Temporal dynamics of surface ocean carbonate chemistry in response to natural and simulated upwelling events during the 2017 coastal El Niño near Callao, Peru, Biogeosciences Discuss. [preprint], https://doi.org/10.5194/bg-2021-111, in review, 2021.

Cline, J. D. and Richards, F. A.: Oxygen deficient conditions and nitrate reduction in the eastern tropical North Pacifc Ocean, Limnol. Oceanogr., 17, 885–900, 1972.

Codispoti, L. A., Yoshinari, T., and Devol, A. H.: Respiration in Aquatic Ecosystems, Suboxic respiration in the oceanic water column, edited by: del Giorgio, P. and Williams, P., Oxford University Press, 2005.

Coplen, T. B., Hopple, J. A., Bölke, J. K., Peiser, H. S., Riedler, S. E., Krouse, H. R., Rosman, K. J. R., Ding, T., Vocke Jr., R. D., Révész, K. M., Lamberty, A., Tayler, P., and De Bièvre, P.: Compilation of Minimum and Maximum Isotope Ratios of Selected Elements in Naturally Occurring Terrestial Materials and

Reagents, U.S. Geological Survey, Water-Resources Investigations Report 01-4222, 2002.

Dalsgaard, T., Canfield, D. E., Petersen, J., Thamdrup, B., and Acuña Gonsález, J.: N_2 production by the anammox reaction in the anoxic water column of Golfo Dulce, Costa Rica, Nature, 422, 606–608, 2003.

Dalsgaard, T., Thamdrup, B., Farías, L., and Revsbech, N. P.: Anammox and denitrification in the oxygen minimum zone of the eastern South Pacific, Limnol. Oceanogr., 57, 1331–1346, 2012.

Dalsgaard, T., De Brabandere, L., and Hall, P. O. J.: Denitrification in the water column of the central Baltic Sea, Geochim. Cosmochim. Ac., 106, 247–260, 2013.

Dalsgaard, T., Stewart, F. J., Thamdrup, B., De Brabandere, L., Revsbech, N. P., Ulloa, O., Canfield, D. E., and DeLong, E. F.: Oxygen at Nanomolar Levels Reversibly Suppresses Process Rates and Gene Expression in Anammox and Denitrification in the Oxygen Minimum Zone off Northern Chile, mBio, 5, e01966–14, https://doi.org/10.1128/mBio.01966-14, 2014.

De Brabandere, L., Canfield, D. E., Dalsgaard, T., Friederich, G. E., Revsbech, N. P., Ulloa, O., and Thamdrup, B.: Vertical partitioning of nitrogen-loss processes across the oxic-anoxic interface of an oceanic oxygen minimum zone, Environm. Microbiol., 16, 3041–3054, 2014.

Deutsch, C., Brix, H., Ito, T., Frenzel, H., and Thompson, L. A.: Climate-Forced Variability of Ocean Hypoxia, Science, 333, 336–339, 2011.

DeVries, T., Deutsch, C., Primeau, F., Chang, B., and Devol, A.: Global rates of water-column denitrification derived from nitrogen gas measurements, Nat. Geosci., 5, 547–550, 2012.

Di Lorenzo, E.: The future of coastal ocean upwelling, Nature, 518, 310–311, 2015.

Espinoza-Morriberón, D., Echevin, V., Colas, F., Tam, J., Ledesma, J., Vásquez, L., and Graco, M.: Impacts of El Niño events on the Peruvian upwelling system productivity, J. Geophys. Res., 122, 5423–5444, 2017.

FAO: The State of World Fisheries and Aquaculture 2018 – Meeting the sustainable development goals, Food and Agriculture Organization of the United Nations, Rome, FAO, 2018.

Farías, L., Castro-González, M., Cornejo, M., Charpentier, J., Faúndez, J., Boontanon, N., and Yoshida, N.: Denitrification and nitrous oxide cycling within the upper oxycline of the eastern tropical South Pacific oxygen minimum zone, Limnol. Oceanogr., 54, 132–144, 2009.

Feely, R. A., Sabine, C. L., Hernandez-Ayon, J. M., Ianson, D., and Hales, B.: Evidence for Upwelling of Corrosive "Acidified" Water onto the Continental Shelf, Science, 320, 1490–1492, 2008.

Fiedler, B., Fietzek, P., Vieira, N., Silva, P., Bitting, H. C., and Körtzinger, A.: In Situ CO_2 and O_2 Measurements on a Profiling Float, J. Atmos. Ocean Technol., 30, 112–126, 2013.

Franco, A. C., Gruber, N., Frölicher, T., and Kropuenske Artman, L.: Contrasting Impact of Future CO_2 Emission Scenarios on the Extent of $CaCO_3$ Mineral Undersaturation in the Humboldt Current System, J. Geophys. Res., 123, 2018–2036, 2018.

Frey, C., Bange, H. W., Achterberg, E. P., Jayakumar, A., Löscher, C. R., Arévalo-Martínez, D. L., León-Palmero, E., Sun, M., Sun, X., Xie, R. C., Oleynik, S., and Ward, B. B.: Regulation of nitrous oxide production in low-oxygen waters off the coast of Peru, Biogeosciences, 17, 2263–2287, https://doi.org/10.5194/bg-17-2263-2020, 2020.

Ganesh, S., Parris, D. J., Delong, E. F., and Stewart, F. J.: Metagenomic analysis of size-fractionated picoplankton in a marine oxygen minimum zone, ISME J., 8, 187–211, 2014.

Ganesh, S., Bristow, L. A., Larsen, M., Sarode, N., Thamdrup, B., and Stewart, F. J.: Size-fraction partitioning of community gene transcription and nitrogen metabolism in a marine oxygen minimum zone, ISME J., 9, 2682–2696, 2015.

Garreaud, R. D.: A plausible atmospheric trigger for the 2017 coastal El Niño, Int. J. Climatol., 38, e1296–e1302, https://doi.org/10.1002/joc.5426, 2018.

Grasshoff, K., Ehrhardt, M., and Kremling, K. (Eds.): Methods of Seawater Analysis. Second, Revised and Extended Edition, Verlag Chemie, Weinheim, Deerfield Beach, 1983.

Hamersley, M. R., Lavik, G., Woebken, D., Rattray, J. E., Lam, P., Hopmans, E. C., Sinninghe Damsté, J. S., Krüger, S., Graco, M., Gutiérrez, D., and Kuypers, M. M. M.: Anaerobic ammonium oxidation in the Peruvian oxygen minimum zone, Limnol. Oceanogr., 52, 923–933, 2007.

Hamme, R. and Emerson, S.: The solubility of neon, nitrogen and argon in distilled water and seawater, Deep-Sea Res. Pt. I, 51, 1517–1528, 2004.

Hauri, C., Gruber, N., McDonnell, A. M. P., and Vogt, M.: The intensity, duration, and severity of low aragonite saturation state events on the California continental shelf, Geophys. Res. Lett., 40, 3424–3428, 2013.

Holtappels, M., Lavik, G., Jensen, M. M., and Kuypers, M. M. M.: Methods in Enzymology, Vol. 486, ^{15}N-Labeling Experiments to issect the Contributions of Heterotrophic Denitrification and Anammox to Nitrogen Removal in the OMS Waters of the Ocean, Elsevier, 223–251, 2011.

Jensen, M. M., Kuypers, M. M. M., Lavik, G., and Thamdrup, B.: Rates and regulation of anaerobic ammonium oxidation and denitrification in the Black Sea, Limnol. Oceanogr., 53, 23–36, 2008.

Jensen, M. M., Petersen, J., Dalsgaard, T., and Thamdrup, B.: Pathways, rates, and regulation of N_2 production in the chemocline of an anoxic basin, Mariager Fjord, Denmark, Mar. Chem., 113, 102–113, 2009.

Jensen, M. M., Lam, P., Revsbech, N. P., Nagel, B., Gaye, B., Jetten, M. S. M., and Kuypers, M. M. M.: Intensive nitrogen loss over the Omani Shelf due to anammox coupled with dissimilatory nitrite reduction to ammonium, ISME J., 5, 1660–1670, 2011.

Junk, G. and Svec, H. J.: The absolute abundance of the nitrogen isotopes in the atmosphere and compressed gas from various sources, Geochim. Cosmochim. Ac., 14, 234–243, 1958.

Kalvelage, T., Jensen, M. M., Contreras, S., Revsbech, N. P., Lam, O., Günter, M., LaRoche, J., Lavik, G., and Kuypers, M. M. M.: Oxygen Sensitivity of Anammox and Coupled N-Cycle Processes in Oxygen Minimum Zones, PLoS One, 6, e29299, https://doi.org/10.1371/journal.pone.0029299, 2011.

Kalvelage, T., Lavik, G., Lam, P., Contreras, S., Arteaga, L., Löscher, C. R., Oschlies, A., Paulmier, A., Stramma, L., and Kuypers, M. M. M.: Nitrogen cycling driven by organic matter export in the South Pacific oxygen minimum zone, Nat. Geosci., 6, 228–234, 2013.

Kämpf, J. and Chapman, P.: Upwelling Systems of the World, chap. The Functioning of Coastal Upwelling Systems, Springer, Switzerland, 2016.

Koeve, W. and Kähler, P.: Heterotrophic denitrification vs. autotrophic anammox – quantifying collateral effects on the oceanic carbon cycle, Biogeosciences, 7, 2327–2337, https://doi.org/10.5194/bg-7-2327-2010, 2010.

Lam, P., Lavik, G., Jensen, M. M., Van Vossenberg, J. D., Schmid, M., Woebken, D., Gutiérrez, D., Amann, R., Jetten, M. S. M., and Kuypers, M. M. M.: Revising the nitrogen cycle in the Peruvian oxygen minimum zone, P. Natl. Acad. Sci. USA, 106, 4752–4757, 2009.

Michiels, C. C., Huggins, J. A., Giesbrecht, K. E., Spence, J. S., Simister, R. L., Varela, D. E., Hallam, S. J., and Crowe, S. A.: Rates and Pathways of N_2 Production in a Persistently Anoxic Fjord: Saanich Inlet, British Columbia, Front. Mar. Sci., 6, 27, https://doi.org/10.3389/fmars.2019.00027, 2019.

Montecino, V. and Lange, C. B.: The Humboldt Current System: Ecosystem components and processes, fisheries, and sediment studies, Progr. Oceanogr., 83, 65–79, 2009.

Oschlies, A., Duteil, O., Getzlaff, J., Koeve, W., Landolfi, A., and Schmidtko, S.: Patterns of deoxygenation: Sensitivity to natural and anthropogenic drivers, Philos. T. R. Soc. A, 375, 20160325, https://doi.org/10.1098/rsta.2016.0325, 2017.

Paulmier, A. and Ruiz-Pino, D.: Oxygen minimum zones (OMZs) in the modern ocean, Progr. Oceanogr., 80, 113–128, 2009.

Paulmier, A., Kriest, I., and Oschlies, A.: Stoichiometries of remineralisation and denitrification in global biogeochemical ocean models, Biogeosciences, 6, 923–935, https://doi.org/10.5194/bg-6-923-2009, 2009.

Peng, X., Fuchsman, C. A., Jayakumar, A., Warner, M. J., Devol, A. H., and Ward, B. B.: Revisiting nitrification in the Eastern Tropical South Pacific: A focus on controls, J. Geophys. Res., 121, 1667–1684, 2016.

Peters, B. D., Babbin, A. R., Lettmann, K. A., Mordy, C. W., Ulloa, O., Ward, B. ., and Casciotti, K. L.: Vertical modeling of the nitrogen cycle in the eastern tropical South Pacific oxygen deficient zone using high-resolution concentration and isotope measurements, Global Biogeochem. Cy., 30, 1661–1681, 2016.

Poornima, D., Shanthi, R., Ranith, R., Srangi, R. K., Saravanakumar, A., and Thangaradjou, T.: Computational Methods for Long Term Monitoring of New Production and f-ratio Variability in Bay of Bengal, Int. J. Ocean. Oceanogr., 14, 109–124, 2020.

Redfield, A. C., Ketchum, B. H., and Richards, F. A.: The influence of organisms on the composition of seawater, in: The Sea, 2nd Edn., edited by: Hill, M. N., Wiley, New York, 26–77, 1963.

Santoro, A., Buchwald, C., Knapp, A., Berelson, W., Capone, D., and Casciotti, K.: Nitrification and Nitrous Oxide Production in the Offshore Waters of the Eastern Tropical South Pacific, Global Biogeochem. Cy., 35, e2020GB006716, https://doi.org/10.1029/2020GB006716, 2021.

Schmid, M. C., Hooper, A. B., Klotz, M. G., Woebken, D., Lam, P., Kuypers, M. M. M., Pommerening-Roeser, A., Op Den Camp, H. J. M., and Jetten, M. S. M.: Environmental detection of octahaem cytochrome c hydroxylamine/hydrazine oxidoreductase genes of aerobic and anaerobic ammonium-oxidizing bacteria, Environ. Microbiol., 10, 3140–3149, 2008.

Schulz, K. G. and Riebesell, U.: Diurnal changes in seawater carbonate chemistry speciation in a high CO_2 world, Mar. Biol., 160, 1889–1899, 2013.

Schulz, K. G., Hartley, S., and Eyre, B. D.: Upwelling Amplifies Ocean Acidification on the East Australia n Shelf: Implications for Marine Ecosystems, Front. Mar. Sci., 6, 636, https://doi.org/10.3389/fmars.2019.00636, 2019.

Stramma, L., Johnson, G. C., Sprintall, J., and Mohrholz, V.: Expanding Oxygen-Minimum Zones in the Tropical Oceans, Science, 320, 655–658, 2008.

Thamdrup, B., Dalsgaard, T., Jensen, M. M., Ulloa, O., Farías, L., and Escribano, R.: Anaerobic ammonium oxydation in the oxygen-deficient waters off northern Chile, Limnol. Oceanogr., 51, 2145–2156, 2006.

Toggweiler, J.: Carbon overconsumption, Nature, 363, 210–211, 1993.

Tyson, R. V. and Pearson, T. H.: Modern and Ancient Continental Shelf Anoxia, Vol. 58, Modern and ancient continental shelf anoxia: an overview, Geological Society Special Publication, 1–24, 1991.

Varela, R., Álvarez, I., Santos, F., deCastro, M., and Gómez-Gesteira, M.: Has upwelling strengthened along worldwide coasts over 1982–2010?, Sci. Rep., 5, 10016, https://doi.org/10.1038/srep10016, 2015.

Vijayaraghavan, S. and Krishna Kumari, L.: Primary production in the southeastern Arabian Sea during southwest monsoon, Ind. J. Mar. Sci., 18, 30–32, 1989.

Wang, D., Gouhier, T. C., Menge, B. A., and Ganguly, A. R.: Intensification and spatial homogenization of coastal upwelling under climate change, Nature, 518, 390–394, 2015.

Wanninkhof, R.: Relationship Between Wind Speed and Gas Exchange Over the Ocean, J. Geophys. Res., 97, 7373–7382, 1992.

Ward, B. B.: How nitrogen is lost, Science, 341, 352–353, 2013.

Ward, B. B., Devol, A. H., Rich, J. J., Chang, B. X., Bulow, S. E., Naik, H., Pratihary, A., and Jayakumar, A.: Denitrification as the dominant nitrogen loss process in the Arabian Sea, Nature, 461, 78–81, 2009.

Yang, S., Gruber, N., Long, M. C., and Vogt, M.: ENSO driven variability of denitrification and suboxia in the Eastern Tropical Pacific Ocean, Global Biogeochem. Cy., 31, 1470–1487, 2017.

Zhang, X., Ward, B. B., and Sigman, D. M.: Global Nitrogen Cycle: Critical Enzymes, Organisms, and Processes for Nitrogen Budgets and Dynamics, Chem. Rev., 120, 5308–5351, 2020.

Zumft, W.: Cell Biology and Molecular Basis of Denitrification, Microbiol. Mol. Biol. Rev., 61, 533–616, 1997.